Journal of Pharmaceutical & Biomedical Analysis
Vol. 1, No. 4, pp. 557–572, 1983
Printed in Great Britain

0731–7085/83 $3.00 + 0.00

Novel applications of multichannel spectroscopy in pharmaceutical analysis*

ANTHONY F. FELL†, BRIAN J. CLARK and HUGH P. SCOTT

Analytical Research Group, Department of Pharmacy, Heriot-Watt University, 79 Grassmarket, Edinburgh, EH1 2HJ, UK

Abstract: Multichannel detectors based on the linear photodiode array, the silicon vidicon tube and charge coupled (or injection) devices are reviewed with reference to their applications in analytical spectroscopy and high-performance liquid chromatography (HPLC). The use of computer-aided techniques, including second derivative spectroscopy and spectral deconvolution methods, for the multichannel spectroscopic analysis of pharmaceuticals is discussed, and applications are reviewed in clinical chemistry, enzyme analysis and studies on aromatic amino acids in proteins. In HPLC, the principles and applications of digital algorithms for validation of peak homogeneity are considered, with reference to spectral suppression, spectral deconvolution, absorbance ratio and the second derivative of the elution profile. The isometric projections of (A, λ, t) data, and their cartographically equivalent contour plots, are discussed and the impact of multicolour graphics is assessed. The implications of two-dimensional multichannel detectors for detection of luminescence radiation are considered in the context of analytical spectroscopy, and detection in both HPLC and thin-layer chromatography. The potential contribution of charge coupled and charge injection devices as the next generation of multichannel detectors is considered.

Keywords: *Multichannel detection; linear photodiode array; silicon vidicon tube; charge coupled device; spectrochromatogram; contour plot; high-performance liquid chromatography; colour graphics; UV-visible spectroscopy; luminescence spectroscopy.*

Introduction

During the past decade the rapid refinement of semiconductor-based technology has led to the evolution of a number of multichannel detector elements, supported by the related development of powerful microprocessor systems. In analytical spectroscopy the most frequently employed multichannel detector is currently the linear photodiode array (LDA), which comprises 200 or more photosensitive diodes. These are usually located in the focal plane of a polychromator diffraction grating (Fig. 1), so that each diode corresponds to a particular wavelength resolution element or 'slice' of the UV-visible

* Presented at the 1st International Symposium on Drug Analysis, June 1983, Brussels, Belgium.
† To whom correspondence should be addressed.

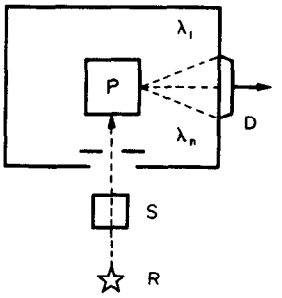

Figure 1
Principles of reversed-optics multichannel detection. R, radiation source; S, sample cell; P, polychromator dispersion radiation from λ_1 to λ_n across surface of multichannel detector D.

spectrum, described by a nominal wavelength [1, 2]. As can be seen from Fig. 1, radiation is passed through the sample cell in 'reversed-optics' configuration.

Whereas the LDA registers information in only one linear dimension, e.g. the wavelength domain, the silicon vidicon tube [1, 2] and the charge coupled device (CCD) or the charge injection device (CID) are characterized by a second linear dimension, since they consist of a two-dimensional lattice of photosensitive elements [3]. This two-dimensional feature can be exploited in a number of ways. For example, a column of diodes can be combined in order to improve the signal-to-noise ratio (SNR) at a particular wavelength element [4]. In another example, a fibre-optic and vidicon tube system has been developed for flame spectroscopy, so that the 'vertical' columns of diodes are used to register information in the vertical flame axis, while each 'horizontal' row of diodes registers the spectrum corresponding to a specific location in the flame [5].

The two-dimensional nature of the silicon vidicon tube has seen elegant exploitation in the work by Christian's group [6, 7] and more recently by Warner's group [8, 9]. In this work, two diffraction gratings are combined orthogonally to form a so-called 'videofluorometer', capable of capturing the entire 'fluorogram'. This is the matrix of fluorescence intensity, I_f, at all permissible values of the excitation wavelength λ_{ex} dispersed in one linear dimension, and of the emission wavelength λ_f, dispersed in the second linear dimension. The emission–excitation matrix (EEM) (I_f, λ_f, λ_{ex}) can be presented graphically as a 3-dimensional isometric display (Fig. 2), or as the cartographically-equivalent contour plot, where all points of equal fluorescent intensity are presented as a contour in the (λ_f, λ_{ex}) plane. It should be noted that it is not necessary to use a two-dimensional multichannel detector in order to obtain the EEM, since conventional computer-aided spectrofluorimeters can acquire this data, albeit more slowly, by scanning the fluorescence spectrum at sequentially-stepped increments of the excitation wavelength, as illustrated in Fig. 2 (B.J. Clark and A.F. Fell, to be published).

Multichannel devices based on silicon photodiodes essentially integrate the incident radiation intensity during a specified observation interval. The minimum interval is determined by the time required to 'read' or interrogate all the photodiode information. In cases where very low radiation intensity is encountered, the elapsed time between each 'reading' can be increased, so that the radiation can be more sensitively detected [2].

Contemporary spectrophotometers incorporating a multichannel detector are almost all based on the LDA. Although silicon vidicon tube detectors are commercially available in modular 'self-assembly' form, they are relatively expensive. For this reason they have not been adopted as the basis of widely-distributed spectrophotometers. Developments involving the CCD and the CID have been restricted to the research

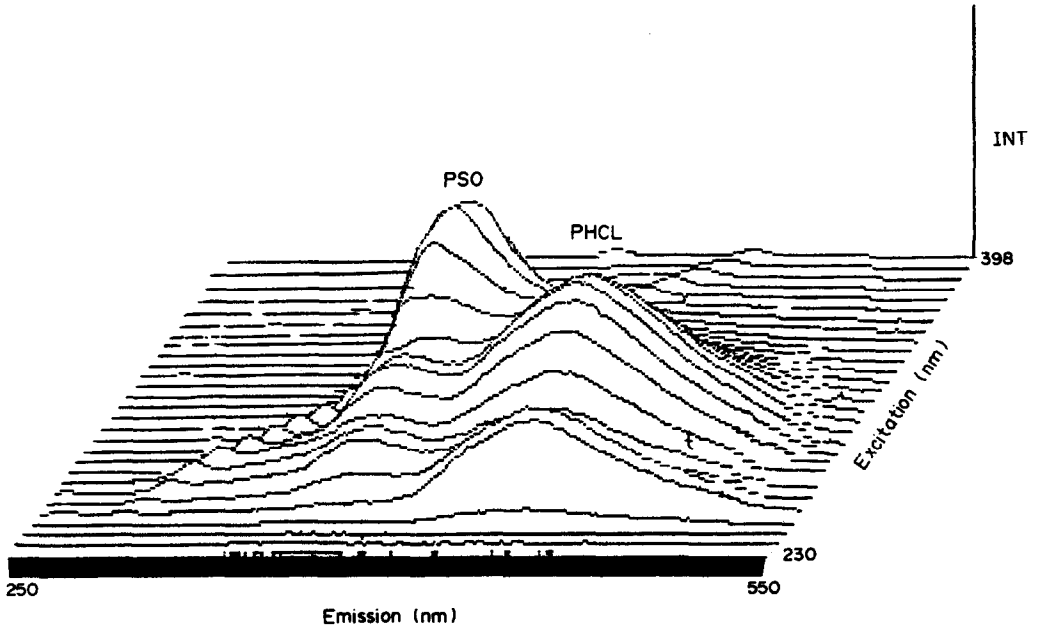

Figure 2
Isometric plot of the emission–excitation matrix of promethazine hydrochloride and its sulphoxide impurity. PHC1, promethazine HC1, 5 μg/ml in phosphate buffer (pH 3.0); PSO, promethazine sulphoxide, 0.48 μg/ml in buffer. Instrumental conditions on Perkin–Elmer LS5 spectrofluorimeter and Model 3600 data station: excitation bandwidth, 5 nm; emission bandwidth, 5 nm; increment in excitation wavelength, 6 nm, for emission monochromator scan speed at 240 nm/min.

literature [3], from which it appears that the utility of these devices has until recently been limited by their relatively low sensitivity below 350 nm. Nevertheless, the intrinsic simplicity of these detectors and their relatively low-cost construction, imply that once the sensitivity-restriction at low wavelength is overcome, the CCD and CID will present an attractive multichannel detector element for the next generation of absorption spectrophotometers, spectrofluorimeters and atomic spectrophotometers.

Multichannel spectrophotometers have recently found application in two key areas of pharmaceutical and biomedical analysis:

(i) rapid-scanning UV-visible absorption spectroscopy; and

(ii) rapid-scanning spectroscopic detection in high-performance liquid chromatography (HPLC).

While it is the aim of this review to indicate the principal types of application in each of these areas, it turns out that the significant novel developments associated with multichannel technology are probably to be found in HPLC. This might have been reasonably anticipated, since the speed of spectral data acquisition in absorption or fluorescence spectroscopy is seldom of concern in itself, unless the observations relate to reaction kinetics or to a highly unstable sample, as for example in the control of photoresist materials used in the semi-conductor industry [10].

In HPLC, on the other hand, as in any dynamic process, the speed of data acquisition is a key factor in determining the overall quality, or time resolution, of the chromatographic elution profile. Moreover, the comparative ease with which UV and in some cases visible spectra can be obtained during elution is in sharp contrast with the

earlier stop-flow methods [11], where the inconvenience of interrupting elution was accompanied by loss of the quantitative information.

In both application areas of multichannel spectroscopy, a significant factor in determining the range and scope of applications has been, and will continue to be, the substantial contribution of computer-aided data processing and graphical presentation techniques available [4, 12–14]. In the present review, the principal digital methods exploited in absorption spectroscopy will be discussed, with particular reference to their novel application in the context of HPLC and other dynamic flow systems.

Principles of Operation of Multichannel Detectors

The main types of multichannel detector, while fundamentally different in construction, share in common the fact that they are based on the properties of a photodiode. In the LDA and the silicon vidicon, the diode is charged to a preset potential and then enabled to respond, usually for a few milliseconds, to incident radiation in the UV to near-IR range, which leads to a progressive loss of charge [1–3]. The photodiode is then interrogated and re-charged to the initial pre-set potential. The charging current required for a diode is proportional to the intensity of radiation integrated by the diode element, and is registered by computer after digitization. In the CCD and its analogue, the charge injection device (CID), the applied potential generates a storage 'well', in which the photogenerated charge is stored before its transfer to a read-out amplifier, as discussed below.

The LDA is a compact device comprising 200 or more photodiodes, in a linear configuration. It is equipped with its own self-scanning circuitry, which permits the status of each photodiode to be interrogated in linear sequence along the array. The analogue signals are gated, digitized and then transmitted via a suitable interface to a microcomputer, where a correction for the 'dark current' and for spectral response profile is made. The spectrum of radiation within a specified range is subtended by the polychromator across the array of photodiodes, each of which corresponds to a defined resolution element, described by a nominal wavelength (Fig. 1). The nominal resolution (in nm/diode) is determined by the dispersion ratio of the polychromator diffraction grating and its geometry relative to the LDA. The resolution could in principle be adjusted, if the polychromator LDA geometry were altered or if the diffraction grating were replaced. The nominal resolution reported for different commercial implementations of the LDA varies from *ca* 0.25 nm to more than 5 nm. Until recently the LDA had to be cooled in order to reduce dark current and thereby attain an acceptable SNR performance [2, 4].

The silicon vidicon, or its more sensitive variant the silicon intensified target (SIT) vidicon [1, 2], consists of a single silicon crystal wafer bearing a microscopic two-dimensional lattice of photosensitive diode junctions. Each diode is selectively interrogated by a continuously scanning electron beam, which performs the charging function described above [1, 2]. The digitized array of intensity data stored by computer is corrected for the 'dark current' and for variations in spectral sensitivity across the surface of the vidicon tube. The SIT differs in having an image intensifier section and phosphor-coated surface built onto the vidicon tube [2]. In addition to the problem of 'blooming' (diode cross-talk) and the need to use Peltier cooling in order to obtain acceptable SNR, the vidicon tube itself is relatively expensive and requires comparatively sophisticated control circuitry for its operation.

Both the CCD and the CID consist of a two-dimensional array of picture resolution elements or 'pixels'. Each CCD pixel is formed by a capacitive 'sandwich', comprising a conductive metal electrode, an insulating layer of SiO_2 and a photosensitive silicon semiconductor. The CCD and CID differ from the LDA in that each pixel accumulates photogenerated charge during illumination [15, 16]. The status of each pixel is interrogated by transferring each discrete 'packet' of charge into an adjacent shift register, where the queue of charge data is read sequentially by a single-readout amplifier [16]. The CID is simpler in construction than the CCD and permits each pixel to be addressed in random access manner, thus enabling electronic selection of specific local areas of the CID surface, analogous to a camera zoom lens [15].

The CCD and CID also differ from the LDA and the silicon vidicon in that the radiation integrated by each pixel is in effect transferred to the read-out device simultaneously. Thus all the pixels report the radiation intensity occurring within the same time interval, whereas the LDA and silicon vidicon detectors require a finite time, $\triangle t$, to scan each of n successive diode elements. Therefore the radiation intensity recorded by the nth diode in the array corresponds to a sampling period which differs by $n\triangle t$ from that for the first diode. Although for many purposes this sampling error may be negligible, there are applications, such as fast reaction kinetics, where this error can introduce spectral distortion.

Although CCD and CID technology have been available for over a decade, relatively few applications have been reported in analytical spectroscopy. These devices have, however, shown very low-noise performance in early studies [3, 16, 17]. However, those devices which are illuminated through the top surface, which carries the metal electrode, have been found to be relatively insensitive below 350 nm. Recently, a version where the lower semiconductor surface has been so thin that it can be illuminated directly, has shown better sensitivity below 350 nm [16].

The types of multichannel detector outlined briefly above represent the principal forms of the technology relevant to analytical spectroscopy. There are a number of other devices, reviewed recently by Talmi [3]. However, by far the most frequently encountered device is the LDA, or its silicon-intensified analogue, which is currently available as a low-noise, inexpensive and sufficiently sensitive element for absorption spectroscopy, where radiation intensity is relatively high. It seems probable that a refined version of the CCD or the CID detector, with back-surface illumination, will offer a low-cost and versatile alternative to the silicon vidicon for applications where the second linear dimension can be exploited.

Applications

The applications of multichannel detectors can be considered under two headings: (i) analytical spectroscopy and (ii) rapid-scanning detection in HPLC. The groups are interrelated in so far as some of the multichannel spectrophotometers currently available for UV-visible spectroscopy can also be used, or converted for use, as detectors in HPLC [13, 14, 18]. Moreover, some digital algorithms developed initially for use in analytical spectroscopy have been found to be especially useful in HPLC, particularly for studies on validation of peak homogeneity, as discussed below.

Analytical spectroscopy

Since the multichannel spectrophotometer is often integrally combined with a

microcomputer, a number of digital functions are available as standard e.g. $\log_{10}$ (absorbance), arithmetic operations on spectra, first and higher order derivatives ($dA/d\lambda$, $d^2A/d\lambda^2$, . . . $d^nA/d\lambda^n$), first and second derivative in the time domain (dA/dt,d^2A/dt^2), Savitzky–Golay smoothing and spectral deconvolution by the principle of overdetermination.

It should be noted that none of these algorithms depends upon the fact than an LDA detector is employed — they are available for use with any computer-aided electromechanically scanning spectrophotometer. The principal difference lies in the speed of spectral registration and in the spectral resolution. While for conventional instruments resolution can be as high as 0.1 nm, for multichannel spectrophotometers the nominal resolution per diode is usually 1–2 nm, although higher resolution instruments are in principle practicable and have been reported, as discussed above. Another feature of the multichannel detector is that spectra can be subjected to ensemble averaging over a period of time in order to improve the SNR.

A recent report described the comparative performance of two algorithms implemented on an LDA-spectrophotometer for the analysis of diphenhydramine hydrochloride (DPH) in a coloured sucrose formulation matrix [14], namely the second derivative and the spectral deconvolution techniques.

The second derivative spectrum of DPH is observed as a series of inverted, sharpened bipolar peaks, corresponding to the aromatic fine structure just discernible in the normal spectrum (Fig. 3). The principle of the second derivative method for the quantitative

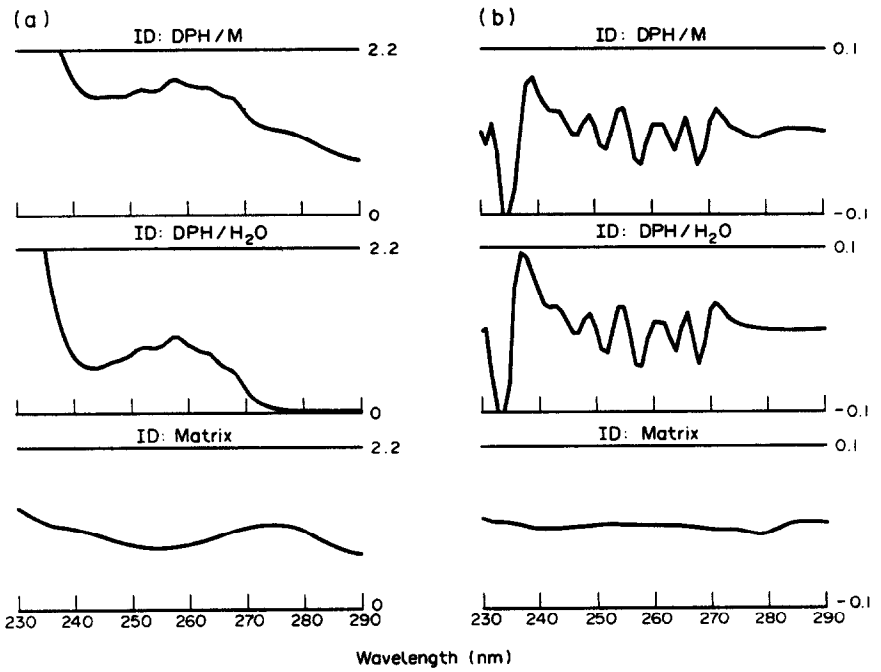

Figure 3
Zero order and second derivative spectra of diphenhydramine hydrochloride by multichannel spectrophotometer. DPH, diphenhydramine HCl (0.624 mg/ml in water); M, formulation matrix diluted (1 + 3) with water; DPH/M, diphenhydramine HCl (0.624 mg/ml) in diluted matrix; (a) zero order UV-spectra; (b) second derivative UV-spectra; Hewlett–Packard HP 8450A, 1 s sampling time [14].

analysis of DPH is that the sharp DPH peaks are selectively enhanced in amplitude, while the broad matrix spectrum is suppressed to an extent which increases in each successive derivative order. Therefore the analyte:matrix ratio of the second derivative amplitudes, D_{2a} and D_{2m}, for a sharp DPH peak a relative to the broad matrix component m at a specified wavelength, varies in inverse ratio to the band widths, W:

$$\frac{D_{2a}}{D_{2m}} = \left[\frac{W_m}{W_a}\right]^2.$$

Thus the amplitude of the peak at 268 nm, measured with respect to the long-wavelength satellite at 271 nm using a multichannel spectrophotometer (Hewlett–Packard HP 8450A, Palo Alto, USA), was shown to be linear with DPH concentration in the range 0–1 mg/ml, with good precision (relative standard deviation, RSD, 0.9%, at 0.683 mg/ml; $n = 8$). In an interaction study using various concentrations of the formulation matrix, the mean recovery of DPH was found to be 101% relative to stoichiometric concentration, indicating effective rejection of the matrix interference [14].

In the spectral deconvolution method, standard spectra for DPH and for the formulation matrix are manipulated by an inverse matrix routine to estimate the concentration of each component according to the principle of 'overdetermination', where the number of wavelength resolution elements exceeds the number of absorbing components in the system. For the DPH formulation, it was found that although good recovery (100.2%) and precision (RSD = 1.3%; $n = 6$) were observed, an interaction study revealed a systematic negative bias in DPH levels with increasing concentration of the formulation matrix. If the reference spectra were transformed to their first derivatives, the deconvolution method reported a mean recovery of 100.1% over the same concentration range (0.2–1.0 mg/ml), with no systematic bias due to the matrix. However, the precision of the derivative deconvolution method was lower than that of the zero order method (RSD = 2.2% at 0.600 mg/ml DPH; $n = 10$).

These examples illustrate the application of just two algorithms which are routinely available on a commercial multichannel UV-visible spectrophotometer. A number of other algorithms based on difference spectroscopy, second derivative–difference spectroscopy and non-linear interpolation could also be exploited using the multichannel spectrophotometer for routine analysis in, for example, quality control laboratories. It should however be borne in mind that in principle all such methods could be implemented using conventional spectrophotometers coupled with a suitable microcomputer, supplied with appropriate software.

Multichannel spectrophotometers have been advocated for a number of years in analytical spectroscopy [1, 19]. In clinical chemistry Pardue's group was among the earliest to demonstrate the utility of the silicon vidicon for clinical estimations of glucose by enzyme-catalyzed reactions, for drugs [20] and for simultaneous enzyme determinations [21]. More recently the LDA spectrophotometer has been applied to the determination of haemoglobin in whole blood using a fibre optic probe [22], and to studies on nonlinear conditions for enzymatic reactions [23]. Other groups have applied the LDA spectrophotometer in stopped-flow kinetic studies on liver alcohol dehydrogenase [24] and to the problem of estimating aromatic amino acid residues in proteins by second derivative spectroscopy [25].

In luminescence spectroscopy, the intensified LDA has been successfully employed to record fluorescence and chemiluminescence spectra in the UV-visible range, for studies

on the kinetics of thiamine oxidation [26]. More recently the same group has extended this work to the analysis of thiamine in pharmaceuticals based on a novel technique exploiting the formation of fluorescent thiochrome under computer-controlled pH-gradient conditions [27]. A more powerful method for multicomponent analysis in clinical chemistry was demonstrated by Christian's group, who exploited the principle of deconvolution applied to the emission–excitation matrix produced by the vidicon-based 'videofluorometer' [6, 7, 28].

Rapid-scanning detection in HPLC

The earliest system for rapid-scanning detection in liquid chromatography was proposed by Bylina *et al.* [29], who developed an ingenious moving-spot oscilloscope as a source of rapidly-scanned spectral radiation. Denton's oscillating mirror spectrometer [30] was demonstrated in studies on uracil, cytosine and adenine. More recently a Russian group developed a similar electromechanical scanning UV-detector for HPLC studies on adenosine phosphates [31]. These devices share the advantage of using a high-sensitivity photomultiplier tube, but require special control to ensure accurate wavelength registration.

By contrast, the multichannel detector is characterized by excellent wavelength registration, but generally lower sensitivity, as shown for the LDA by a number of groups [4, 32, 33] and for the silicon vidicon [34–36].

More recently, high-performance, low-noise LDA spectrophotometers have been commercially developed and applied in HPLC. These permit spectra to be readily obtained for confirmation of identity and have found application in forensic toxicology for drug screening programmes [37] and in environmental toxicology for the analysis of drug dust residues, both directly and with the use of spectral deconvolution [38].

Studies on drug metabolism have recently exploited the LDA detector for confirmation of identity [39–41] and as a tool for examining the stability of butoprozine metabolites extracted from dog bile [42]. In these studies the use of three-dimensional 'spectrochromatograms' of (A, λ, t) as pseudoisometric plots was advocated as a rapid and successful means for visually assessing the optimum strategy for method development in toxicological investigations.

However, an alternative graphical presentation proposed recently is to reduce the (A, λ, t) data to a contour plot, comprising a series of concentric isoabsorptive lines mapped in the (λ, t) plane [43]. This is the cartographic equivalent of the three-dimensional isometric plot (Fig. 4) and has the property that all components in the spectrochromatogram that are above the threshold minimum can be visualized simultaneously. By contrast, it is necessary to rotate the isometric plot about a vertical axis in order to examine areas of the data which may be obscured by larger foreground peaks. Non-homogeneity of a chromatographic peak can be sometimes indicated in the contour plot by asymmetry in the shape of the contour lines, as can be seen for the overlapping *N*-oxide (III) and hydroxy-metabolite (IX) of zimeldine, illustrated in Fig. 5.

The contour plot can be readily used to establish the optimum detection wavelength for each peak [43]. The chromatogram can be presented at a number of wavelengths simultaneously, each selected in order to optimize the sensitivity for each component [13, 18, 43–45].

The wavelength data can in fact be manipulated digitally in a number of ways to give enhanced selectivity and sensitivity. For example, if the absorbances of all the wavelength resolution elements are summed, a total absorbance chromatogram is

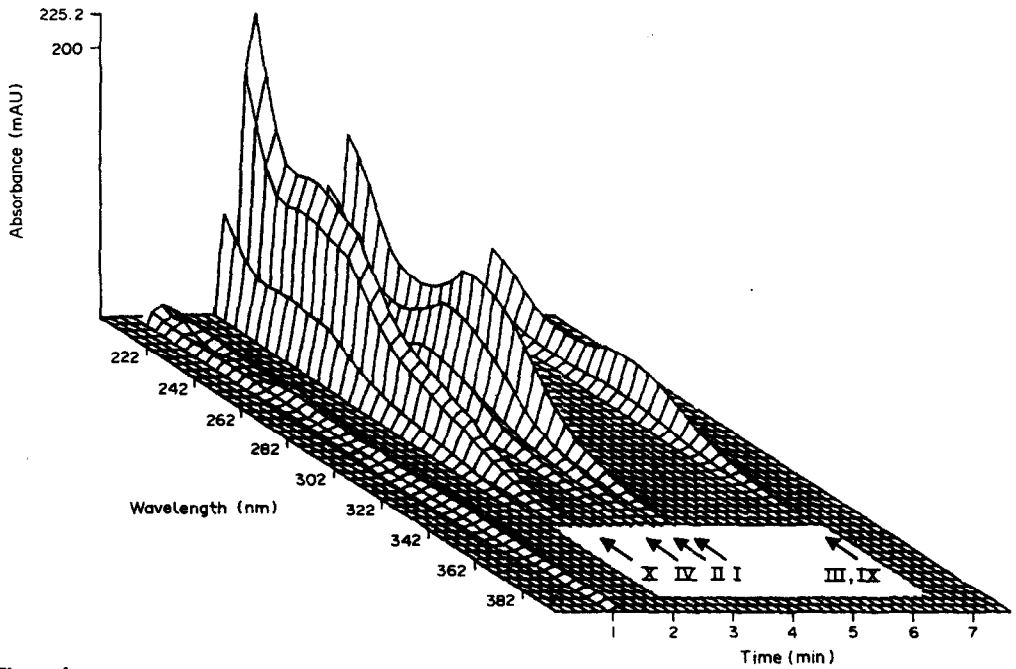

Figure 4
Isometric plot of spectrochromatogram of zimeldine and metabolites separated by reversed-phase HPLC. I, zimeldine (32.9 μg/ml in distilled water); II, norzimeldine (23.6 μg/ml); III, zimeldine *N*-oxide (30.9 μg/ml); IV, desmethyl zimeldine (28.9 μg/ml); IX, zimeldine hydroxylamine (19.3 μg/ml); Z, E-isomer of norzimeldine (16.0 μg/ml); injection volume, 20 μl. Instrumental conditions for Hewlett–Packard HP 1040A photodiode array detector and HP85 microcomputer: bandwidth at detection wavelength, 4 nm; bandwidth at reference wavelength (550 nm), 100 nm; spectral acquisition rate, 1 s^{-1}; observation angle 35°C viewed from the left. Chromatographic conditions as in [49].

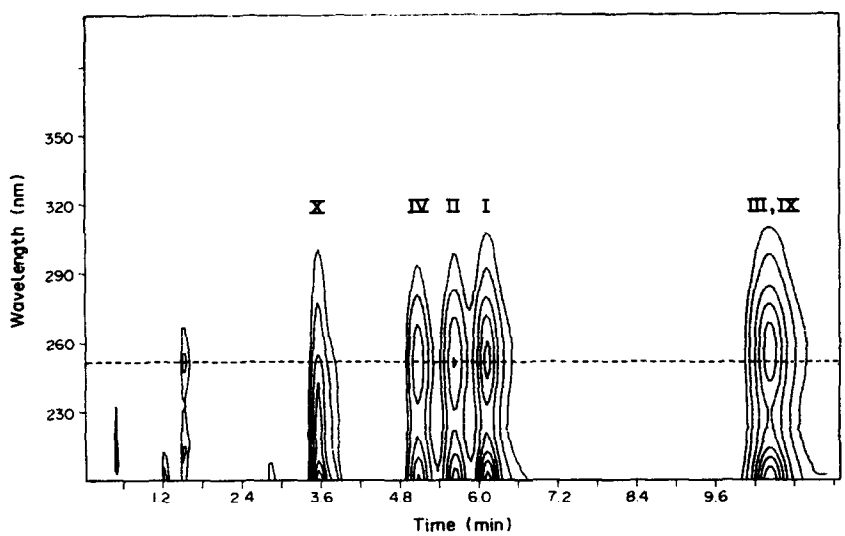

Figure 5
Contour plot of zimeldine and metabolites separated by reversed-phase HPLC. Contour intervals: 10, 25, 50, 100, 125, 150, 175, 200 a.u. Optimum detection wavelength *ca* 250 nm for I, II, III, IV and IX; key to solutes as in Fig. 4. Instrumental conditions for Hewlett–Packard HP 1040A photodiode array detector and HP85 microcomputer as in Fig. 4; chromatographic conditions as in [49].

obtained which, analogously to total ion current in mass spectrometric LC-detection, presents a global indication of all components present, which could be useful for detecting minor impurities [43]. Sensitivity can be increased by grouping the output of adjacent diodes together ("diode bunching") and/or by co-addition of sequential points in the elution profile [43]. Another algorithm proposed to aid confirmation of identity is to transform the individual spectra to the corresponding second or higher derivative in the wavelength domain ($d^2A/d\lambda^2$, . . .) [13, 44, 46].

A number of digital algorithms have recently been proposed for assessing the homogeneity of a chromatographic peak by rapid-scanning detection [38, 43–47]. The absorbance ratio at two carefully chosen wavelengths, plotted as a function of elution time, gives an indication of non-homogeneity as a discontinuity in the plot, provided that the spectral properties of the overlapping solutes are sufficiently different [18, 44]. Comparison of normalized spectra captured at the apex and on the leading and trailing edges of the peak has also been found to give a sensitive indication of impurity [12].

The second or higher derivative of the elution profile at a specified wavelength (d^2A/dt^2, . . .) has recently been shown to give resolution of overlapping peaks [43, 45, 48], due to the now well-established band-sharpening effect [46]. The technique has the merit that the overlapping components do not require to have different spectra. However, in common with the absorbance ratio and spectral normalization methods, the derivative technique requires that the overlapping components have retention times differing by a minimum interval. The second derivative method has been found to be a sufficiently sensitive criterion for use in the automated optimization of chromatographic separation in the pharmaceutical industry [48].

The method of spectral suppression recently proposed for peak purity validation [47] utilizes difference spectroscopy to suppress selectively the chromatographic peak of a known component, thereby revealing any co-eluting impurity peak or peaks [45]. This method essentially relies on the principle that the absorptivity of a pure component at one wavelength is in fixed proportion to that at another:

$$\epsilon_{\lambda 1} = K_{1,2} \cdot \epsilon_{\lambda 2} \tag{1}$$

so that at any concentration within the linear range, the absorbance relationships are:

$$A_{\lambda 1} = K_{1,2} \cdot A_{\lambda 2}. \tag{2}$$

Thus the absorbance contribution of the pure component can be suppressed by computing, as a function of time, the difference function:

$$\Delta A_{1,2} = A_{\lambda 1} - K_{1,2} \cdot A_{\lambda 2} = 0. \tag{3}$$

In the simplest case, the wavelengths λ_1 and λ_2 correspond to equiabsorptive points in the spectrum, so that $K_{1,2}$ is unity.

In the example of zimeldine (I) and its closely related metabolites norzimeldine (II) and the desmethyl compound (IX), analysed by reversed-phase ion-pair chromatography on 5- μm C_{18}-Nucleosil with acetonitrile-buffer as previously described [43, 49], the UV-spectra are very closely similar. Although their absorption maxima differ by only about 1 nm (Fig. 6), it has been found that by computing an optimized difference absorbance ΔA for 240 and 260 nm, each of the three overlapping components can be selectively

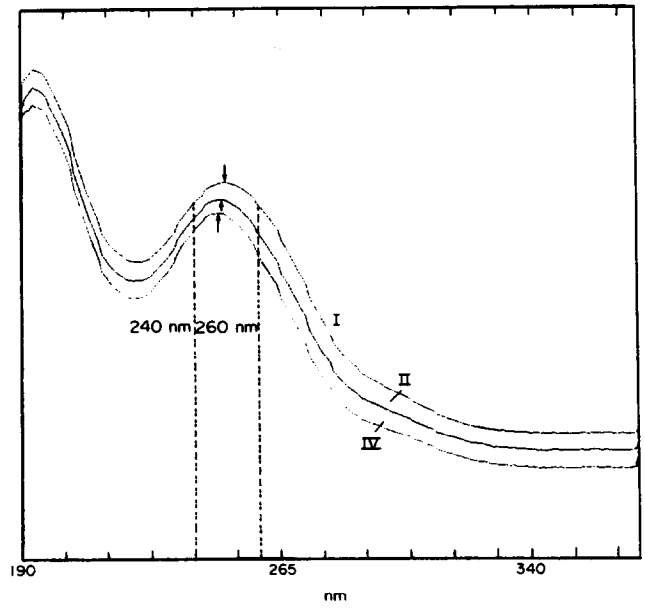

Figure 6
Normalized UV-spectra of zimeldine and metabolites acquired during separation by reversed-phase HPLC. I, zimeldine; II, norzimeldine; IV, desmethyl zimeldine; injection volume 20 μl; spectra normalized and off-set by *ca* 0.05 a.u. Arrows indicate spectral maxima; 240 nm, 260 nm, represent optimum wavelengths for spectral suppression. Instrumental conditions for the LKB 2140 photodiode array rapid spectral detector and IBM-PC microcomputer: bandwidth at detection wavelength, nominally 4 nm; integration (sampling) time, 1 s. Chromatographic conditions as in [49].

suppressed [43], as indicated in Fig. 7, where the regular chromatogram (green) is compared with the spectral suppression chromatograms (red) for each component. Thus a co-eluting impurity can be detected, provided that it is characterized by a UV-spectrum which differs sufficiently from the spectrum of the suppressed component, and that the product ($\Delta\varepsilon.c$) of its concentration c is higher than the SNR.

The case of zimeldine and its metabolites illustrates the need to carefully optimize the values of $K_{1,2}$, λ_1 and λ_2, using an interactive programme operating on stored spectrochromatograms obtained once only for each component, as indicated in Fig. 7. The selectivity observed between zimeldine and these two principal metabolites is remarkable, and confirms the potential utility of spectral suppression for peak homogeneity validation, after suitable optimization [45, 47].

A number of other techniques are available to assess chromatographic peak purity. One, spectral deconvolution, suffers from the disadvantage that reference spectra for each co-eluting component are required *a priori*, although in some cases it may be possible to cope with an uncharacterized co-eluting component if it elutes on the leading or trailing edge of the peak, as shown recently in a study on the papaverine and noscapine peaks in a sample of heroin [45]. Principal component analysis should offer a potentially powerful method in cases where the number of components in a spectrochromatogram is unknown [50–52].

Further applications of rapid scanning HPLC detection can be anticipated with archive retrieval methods, based either on zero order or on derivative spectra, as developed recently for limited libraries of compounds (H.P. Scott, A.F. Fell, to be published). This approach encounters a number of difficulties, not least of which is the effect of different eluents on the spectra of ionizable and other solutes. It seems advisable, therefore, that individual archives should be established on the basis of standardized eluent systems. In method optimization, rapid-scanning detection coupled with archive retrieval will also prove useful in assigning identity to peaks whose elution order may vary during the process of optimization.

Development Trends

The advent of 16-bit and 32-bit microcomputers in the analytical laboratory has made it possible to consider a number of data processing techniques for greater selectivity and sensitivity in spectroscopy and in HPLC detection. Principal component analysis and archive retrieval techniques can now be complemented by methods such as cluster analysis and pattern recognition [53–55].

Interactive graphics have become a practicable tool in method development, as discussed above. Moreover, multi-colour graphics can now be used to represent additional information levels as illustrated in Fig. 8, where the three-dimensional contour plane is coded in eight colours to represent the shape and location of the peaks of interest. The use of colour graphics, well established in certain branches of experimental science, has recently become a routinely available option in HPLC [56]. Discussion will probably continue as to the relative merits of colour versus conventional black–white graphics (cf Figs 5 and 8, where each plot represents the same drug and metabolite data).

The use of the silicon vidicon for fluorimetric detection in HPLC may well be overtaken by the CCD or the CID as a less expensive two-dimensional alternative. The potential of such detectors for sensitive and selective luminescence detection in biomedical applications has already been established in the research environment by a number of groups using the vidicon-detector [6–9, 57, 58].

Indeed, the use of two-dimensional multichannel photometric detectors has already been demonstrated in other areas of analysis, such as TLC, where the separation of phenylporphine derivatives was presented as a novel three-dimensional isometric plot of (I_f,λ_f,d), i.e. fluorescence intensity (I_f) as a function of emission wavelength (λ_f) and elution distance (d) [59, 60]. It is to be anticipated that CCD technology may soon make such devices commercially attractive.

Clearly the multichannel spectrophotometric detector has significant potential for a number of dynamic flow systems other than HPLC. For example, there are a number of interesting applications in flow-injection analysis [61] which could well benefit from the incorporation of a computer-aided rapid-scanning UV-detector.

More generally, multichannel detection in HPLC and other flow systems is not limited to photometric principles. For example, there is now a new generation of multichannel glassy-carbon electrochemical detectors, which are capable of recording the cyclic voltammogram as a function of time under dynamic flow conditions [62]. It remains a matter for speculation as to what extent the next generation of multichannel detector elements will continue to transform the face of analytical technology in the biomedical sciences, as the evolution of powerful microcomputers proceeds.

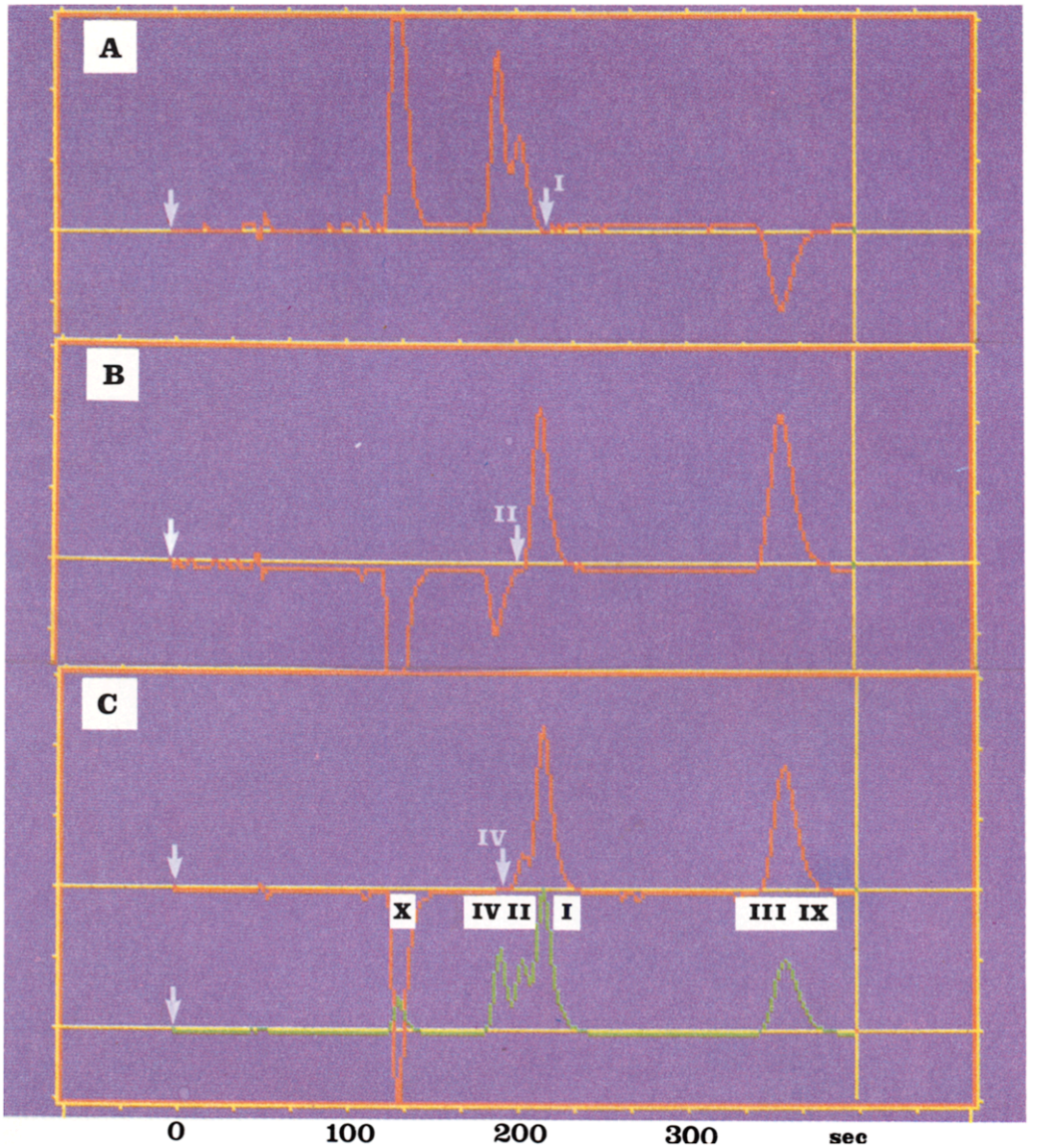

Figure 7
Selective spectral suppression of zimeldine and metabolites by photodiode array detection in HPLC. For key to solutes, see Fig. 4; chromatographic conditions as in [49]. A, suppression of zimeldine (I): $\Delta A = A_{240} - 1.041\ A_{260}$. B, suppression of norzimeldine (II): $\Delta A = A_{260} - 0.852\ A_{240}$. C, suppression of desmethyl zimeldine (IV): $\Delta A = A_{260} - 0.897\ A_{240}$; conventional chromatogram (green) at 250 nm. Instrumental conditions for the LKB 2140 photodiode array rapid spectral detector and IBM-PC microcomputer, as in Fig. 6.

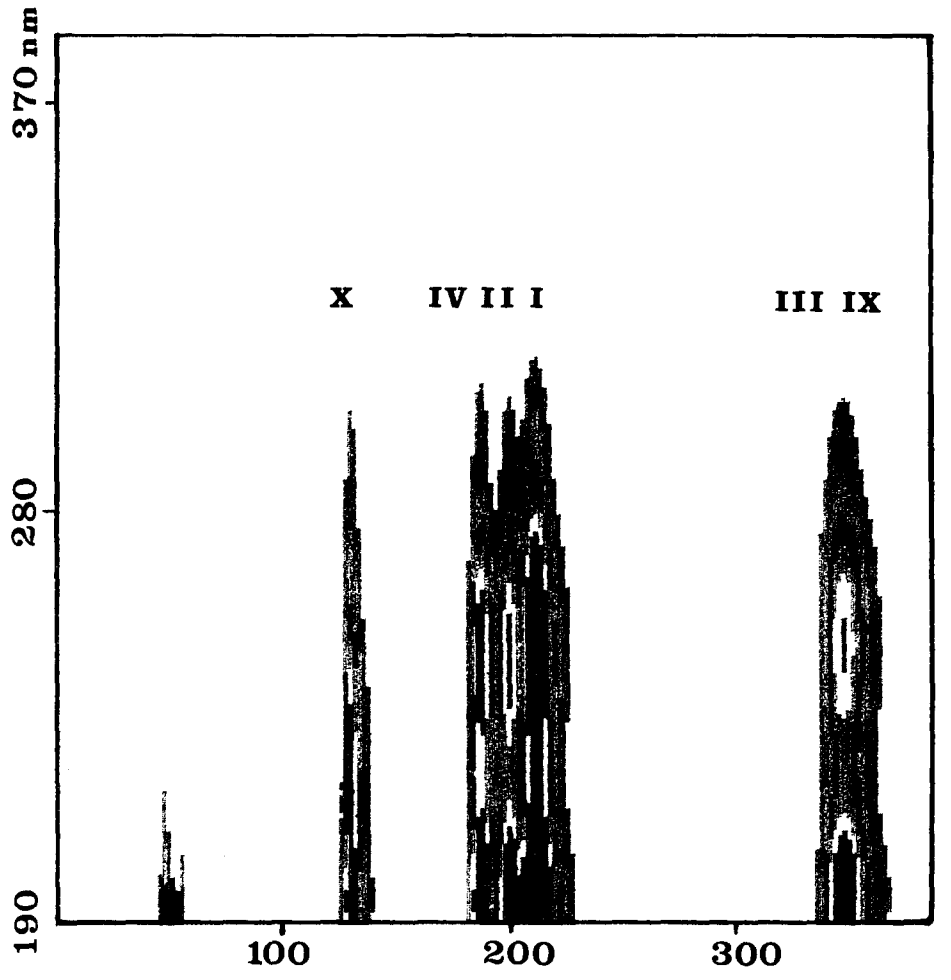

Figure 8
Colour-coded contour plot of zimeldine and metabolites separated by reversed-phase HPLC. For key to solutes, see Fig. 4. Contour intervals: black/grey, 0; cyan blue, 0.02 a.u.; blue, 0.03 a.u.; green, 0.04 a.u.; yellow, 0.05 a.u.; red, 0.06 a.u.; magenta, >0.07 a.u.; maximum sensitivity, 0.1 a.u.f.s. Instrumental conditions for the LKB 2140 photodiode array rapid spectral detector and IBM-PC microcomputer with Canon 8-colour ink-jet plotter: as in Fig. 6. For chromatographic conditions, see [49].

Acknowledgements: We thank Dr Douglas Westerlund, Mrs Ewa Erixson, Dr Jan Lundström and colleagues at Astra Läkemedel AB, Södertälje, Sweden, for valuable and stimulating discussions, during some of this work. The use of a Model HP 1040A photodiode array detector and peripherals kindly supplied by Hewlett–Packard GMBH, Waldbronn, F.R.G., is acknowledged with thanks. Thanks are also extended to LKB Produkter AB, Bromma, Sweden, for access to a Model 2140 rapid spectral detector and peripherals. The Home Office, London, U.K. is thanked for a research fellowship to one of us (H.P.S.). Thanks are extended to Dr Richard Gill and Dr Anthony C. Moffat at the Central Research Establishment, Home Office Forensic Science Service, Aldermaston, U.K. for valuable and provocative discussions throughout this work.

References

[1] R. E. Santini, M. J. Milano and H. L. Pardue, *Anal. Chem.* **45**, 915A–927A (1973).
[2] Y. Talmi, Ed., *Multichannel Image Detectors*, ACS Symp. Ser. No. 102. American Chemical Society, Washington, DC. (1979).
[3] Y. Talmi, *Anal. Chem.* **47**, 697A–709A (1975).
[4] M. J. Milano, S. Lam, M. Slavonis, D. B. Pautler, J. W. Pav and E. Grushka, *J. Chromatogr.* **149**, 599–614 (1978).
[5] K. W. Busch, B. Malloy and Y. Talmi, *Anal. Chem.* **51**, 670–673 (1979).
[6] I. M. Warner, J. B. Callis, E. R. Davidson, R. Gouterman and G. D. Christian, *Anal. Lett.* **8**, 665–681 (1975).
[7] D. W. Johnson, G. A. Gladden, J. B. Callis and G. D. Warner, *Rev. Sci. Instrum.* **50**, 118–126 (1979).
[8] M. P. Fogarty, D. C. Shelly and I. M. Warner, *J. High Resolut. Chromatogr. Chromatogr. Commun.* **4**, 561–568 (1981).
[9] D. C. Shelley, M. P. Fogarty and I. M. Warner, *J. High Resolut. Chromatogr. Chromatogr. Commun.* **4**, 616–626 (1981).
[10] H. T. Wu, UV-Vis Application Note AN-295-2. Hewlett-Packard, Palo Alto, California (1980).
[11] A. M. Krstulovic, R. A. Hartwick, P. R. Brown and K. Lohse, *J. Chromatogr.* **158**, 365–376 (1978).
[12] S. A. George and A. Maute, *Chromatographia* **15**, 419–425 (1982).
[13] A. F. Fell, H. P. Scott, R. Gill and A. C. Moffat, *Chromatographia* **16**, 69–78 (1982).
[14] A. F. Fell, H. P. Scott, R. Gill and A. C. Moffat, *Anal. Proc.* **20**, 173–176 (1983).
[15] H. A. Lewis and M. B. Denton, *J. Automat. Chem.* **3**, 9–12 (1981).
[16] G. D. Christian, J. B. Callis and E. R. Davidson, in *Modern Fluorescence Spectroscopy* (E. L. Wehry, Ed.), Vol. 4, pp. 111–165. Plenum Press, New York (1981).
[17] K. L. Ratzlaff and S. L. Paul, *Appl. Spectrosc.* **33**, 240–245 (1979).
[18] G. E. James, *Can. Res.* **13**, 39–43 (1980).
[19] H. L. Pardue, *Top. Automat. Chem. Anal.* **1**, 163–207 (1979).
[20] H. L. Pardue, A. E. McDowell, D. M. Fast and M. J. Milano, *Clin. Chem. (Winston-Salem, N.C.)* **21**, 1192–1200 (1975).
[21] M. J. Milano and H. L. Pardue, *Clin. Chem. (Winston-Salem, N.C.)* **21**, 211–215 (1975).
[22] M. J. Milano and K.-Y. Kim, *Anal. Chem.* **49**, 555–559 (1977).
[23] S. D. Hamilton and H. L. Pardue, *Clin. Chem. (Winston-Salem, N.C.)* **28**, 2359–2365 (1982).
[24] S. C. Koerber and M. F. Dunn, *Biochimie* **63**, 97–102 (1981).
[25] R. M. Levine and M. M. Federici, *Biochemistry* **21**, 2600–2606 (1982).
[26] M. A. Ryan, R. J. Miller and J. D. Ingle, *Anal. Chem.* **50**, 1772–1777 (1978).
[27] M. A. Ryan and J. D. Miller, *Talanta* **28**, 225–231 (1981).
[28] I. M. Warner, J. B. Callis, E. R. Davidson and G. D. Christian, *Clin. Chem. (Winston-Salem, N.C.)* **22**, 1483–1492 (1976).
[29] A. Bylina, D. Sybilska, Z. R. Grabowski and J. Koszewski, *J. Chromatogr.* **83**, 357–362 (1973).
[30] M. S. Denton, T. P. DeAngelis, A. M. Yacynych, W. R. Heineman and T. W. Gilbert, *Anal. Chem.* **48**, 20–24 (1976).
[31] G. I. Baram, M. A. Grachev *et al.*, *J. Chromatogr.* **264**, 69–90 (1983).
[32] M. J. Milano, S. Lam and E. Grushka, *J. Chromatogr.* **125**, 315–326 (1976).
[33] R. E. Dessy, W. D. Reynolds *et al.*, *J. Chromatogr.* **126**, 347–368 (1976).
[34] A. E. McDowall and H. L. Pardue, *Anal. Chem.* **48**, 1815–1816 (1976).
[35] A. E. McDowall and H. L. Pardue, *Anal. Chem.* **49**, 1171–1176 (1977).
[36] L. N. Klatt, *J. Chromatogr. Sci.* **17**, 225–235 (1979).
[37] P. M. Kabra, B. E. Stafford and L. J. Marton, *J. Anal. Toxicol.* **5**, 177–182 (1981).
[38] C. J. Warwick and D. A. Bagon, *Chromatographia* **15**, 443–436 (1982).
[39] B. F. H. Drenth, R. T. Ghijsen and R. A. de Zeeuw, *J. Chromatogr.* **238**, 113–120 (1982).
[40] F. Overzet, R. T. Ghijsen, B. F. H. Drenth and R. A. de Zeeuw, *J. Chromatogr.* **240**, 190–195 (1982).
[41] R. T. Ghijsen, B. F. H. Drenth, F. Overzet and R. A. de Zeeuw, *J. High Resolut. Chromatogr. Chromatogr. Commun.* **5**, 192–198 (1982).
[42] F. Overzet, *J. High Resolut. Chromatogr. Chromatogr. Commun.* **5**, 604–615 (1982).

[43] B. J. Clark, A. F. Fell, H. P. Scott and D. Westerlund, *J. Chromatogr.* **286**, 271–283 (1984).
[44] A. F. Fell, H. P. Scott, R. Gill and A. C. Moffat, *J. Chromatogr.* **273**, 3–17 (1983).
[45] A. F. Fell, H. P. Scott, R. Gill and A. C. Moffat, *J. Chromatogr.* **282**, 123–140 (1983).
[46] A. F. Fell, *Anal. Proc.* **17**, 512–519 (1980).
[47] G. T. Carter, R. E. Schiesswohl, H. Burke and R. Yang, *J. Pharm. Sci.* **71**, 317–321 (1982).
[48] J. C. Berridge, *Chromatographia* **16**, 172–174 (1982).
[49] D. Westerlund and E. Erixson, *J. Chromatogr.* **185**, 593–603 (1979).
[50] J. M. Halket, *J. High Resolut. Chromatogr. Chromatogr. Commun.* **2**, 197–198 (1979).
[51] M. McCue and E. R. Malinowski, *J. Chromatogr. Sci.* **21**, 229–234 (1983).
[52] E. R. Malinowski and D. G. Howery, *Factor Analysis in Chemistry*. Wiley, New York (1981).
[53] D. L. Massart, *Cluster Analysis*. Elsevier, Amsterdam (1982).
[54] L. Kryger, *Talanta* **28**, 871–887 (1981).
[55] B. R. Kowalski, *Trends Anal. Chem.* **1**, 71–74 (1981).
[56] A. F. Fell, B. J. Clark and H. P. Scott, *J. Chromatogr.* (in press).
[57] L. W. Hershberger, J. B. Callis and G. D. Christian, *Anal. Chem.* **53**, 971–975 (1981).
[58] T. M. Rossi, J. M. Quarles and I. M. Warner, *Anal. Lett.* **15**, 1083–1098 (1982).
[59] M. L. Gianelli, J. B. Callis, N. H. Anderson and G. D. Christian, *Anal. Chem.* **53**, 1357–1361 (1983).
[60] M. L. Gianelli, D. H. Burns, G. D. Christian and N. H. Anderson, *Anal. Chem.* **55**, 1858–1862 (1983).
[61] J. Ružička and E. H. Hansen, *Flow Injection Analysis*. Wiley, New York (1981).
[62] W.L. Caudill, A. G. Ewing, S. Jones and R. M. Wightman, *Anal. Chem.* **55**, 1877–1881 (1983).

[Received 10 June 1983]